Nonlinear Optics (WiSe 2017/18)
Lecture 15: December 7, 2017

Continue 9 Optical Parametric Amplifiers and Oscillators

9.9 Ultrabroadband optical parametric amplifiers
using noncollinear phase matching

9.10 Optical parametric chirped-pulse amplification (OPCPA)

9.8   Noncollinear optical parametric amplifier (NOPA)

9.9   Optical parametric chirped-pulse amplification (OPCPA)

9.9.1   Temporal optimization of ultrabroadband high-energy OPCPA

[5] Largely follows the review paper by G. Cerullo *et al.*, "Ultrafast Optical Parametric Amplifiers," Rev. Sci. Instrum. 74, 1-17 (2003)

Noncollinear OPA (NOPA)
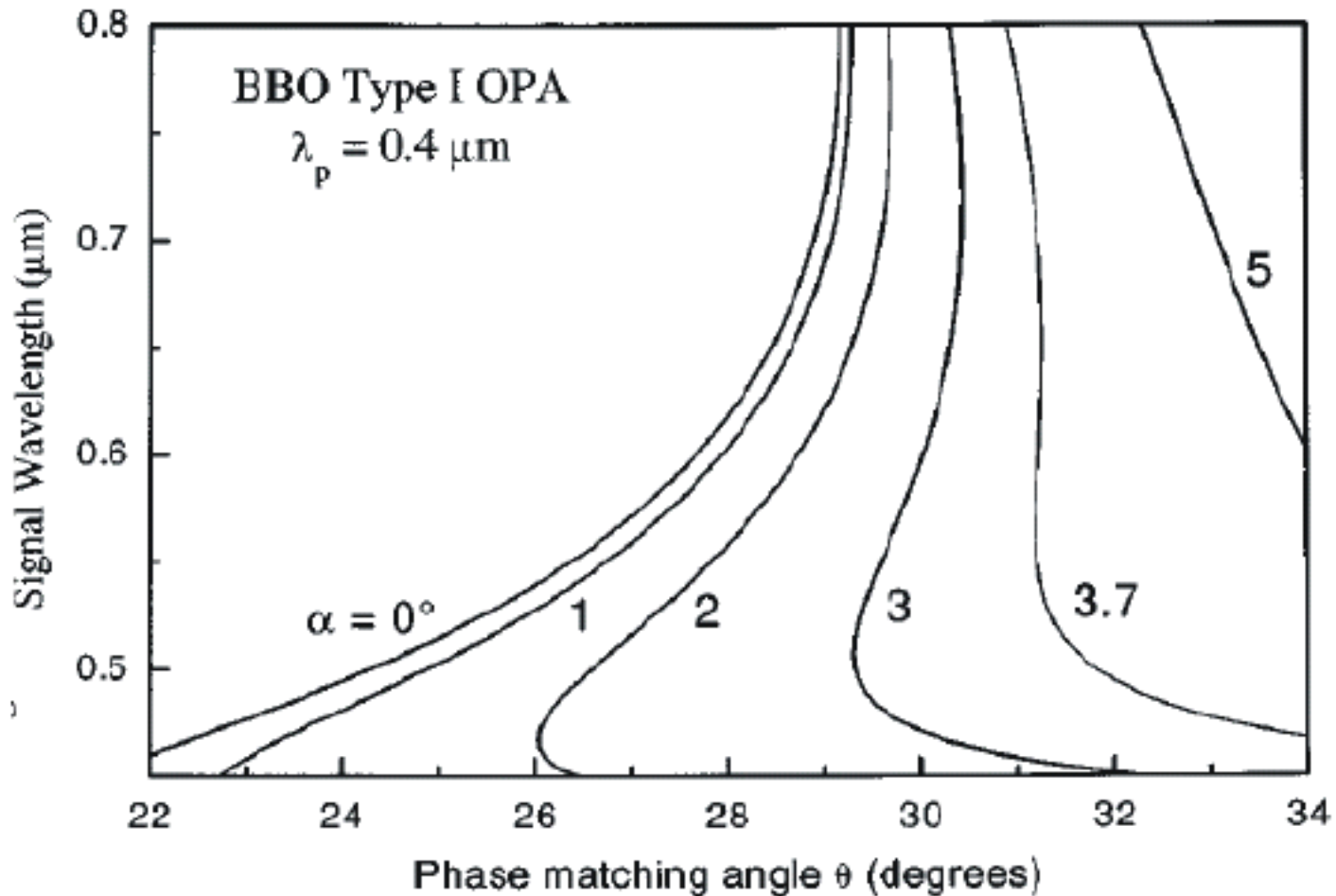
Fig. 9.18: Phase-matching curves for a noncollinear type-I BBO OPA pumped at λ_p=0.4 µm, as function of the pump-signal angle α. [5]

NOPA Layout
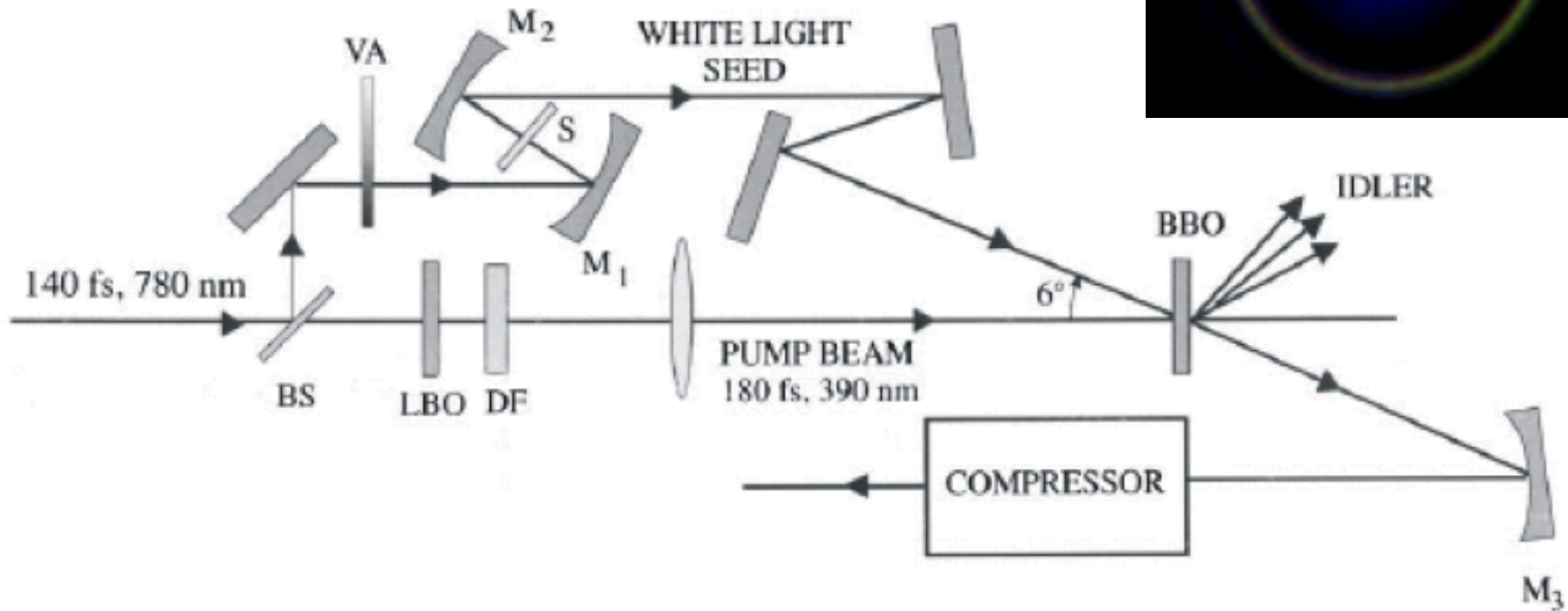
Figure 9.19: Scheme of a noncollinear visible OPA. BS: beam splitter; VA: variable attenuator; S: 1-mm-thick sapphire plate; DF: dichroic filter; M1 ,M2 , M3 , spherical mirrors.[5]

pulse-front matched parametric interaction geometry

R. Danielius *et al.*, Opt. Lett. **21**, 973 (1996)
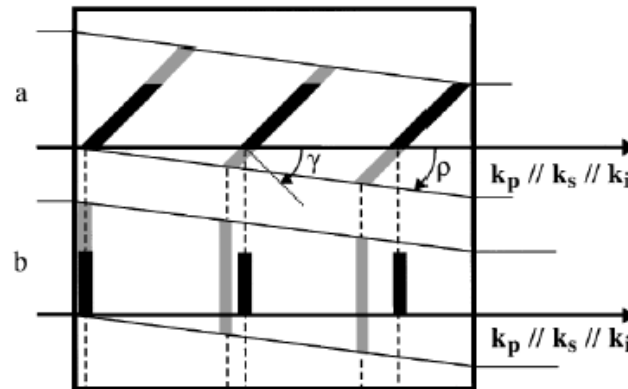
Figure 9.22: Effects of the pump-pulse wavefront tilt on group-velocity mismatch (GVM) in a collinear type-I OPA: (a) tilted pump pulses for a suitable tilt angle γ, where the fast signal pulse (thick solid lines) propagates under the slow pump (thick grey lines) because of the walk-off contribution to collinear group velocity (ρ, birefringent walk-off angle); (b) untilted pump pulses. From [8].
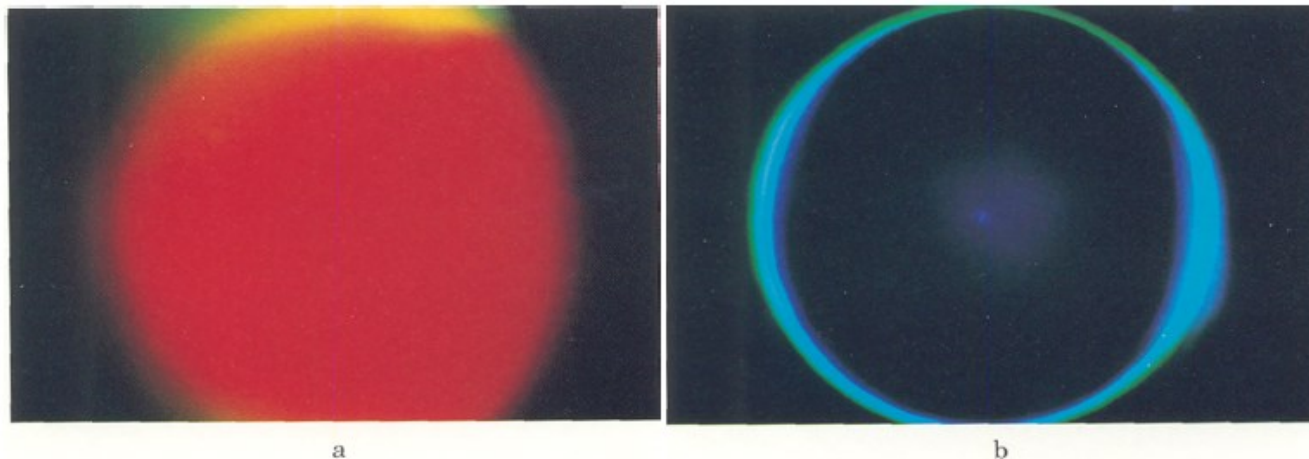
Figure 9.23: Photos of the parametric superfluorescence for a given crystal orientation for (a) tilted and (b) untilted 100-fs 0.4-μm pump pulses. From [8].

4

type-I NOPA: pump e beam, signal and idler are o

$\rightarrow$ group velocities of signal and idler not affected by tilting

Figure 9.24: Front-tilted pumping of a type-I NOPA. α_{ext} is the external non-collinearity angle between the pump and signal. The tilt angle generated by the prism is γ_{prism}, the tilt angle imaged into the crystal is γ_{int}. From [9].
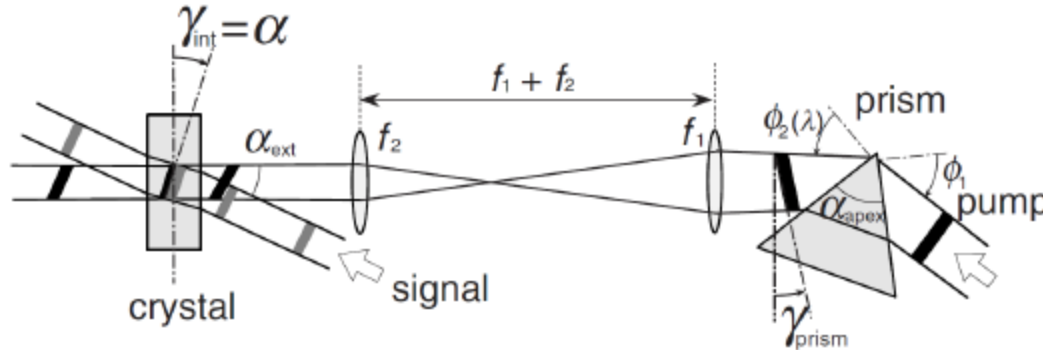
A. Baltuška and T. Kobayashi, Meas. Sci. Technol. **13**, 1671 (2002)

Therefore this technique can also be used to improve the amplified signal pulse properties, as sketched in Fig. 9.24: The pump beam passes through a prism with apex angle α_{apex}, at incident angle ϕ_1 and exit angle $\phi_2(\lambda)$. Directly after the prism, the pulse-front tilt angle is given by

$$\tan \gamma_{\mathrm{prism}} = -\lambda_p \frac{\mathrm{d}\phi_2}{\mathrm{d}\lambda_p} = -\frac{\sin \alpha_{\mathrm{apex}}}{\cos \phi_1' \cos \phi_2} \lambda_p \frac{\mathrm{d}n}{\mathrm{d}\lambda_p}, \qquad (9.47)$$

with the refractive index of the prism n and ϕ_1' the angle of refraction. The angle γ_{prism} is then imaged onto the crystal position to an angle γ_{ext} using a telescope with lenses f_1 and f_1 resulting in a magnification factor f_1/f_2. The

type-I NOPA: pump e beam, signal and idler are o

→ group velocities of signal and idler not affected by tilting

Figure 9.24: Front-tilted pumping of a type-I NOPA. α_{ext} is the external non-collinearity angle between the pump and signal. The tilt angle generated by the prism is γ_{prism}, the tilt angle imaged into the crystal is γ_{int}. From [9].

internal tilt angle γ_{int} is then reduced due to refraction by v_p/c. Thus the condition for pulse-front matching, $\gamma_{\text{int}} = \alpha$, leads to

$$\tan \alpha = \frac{v_p}{c} \frac{f_1}{f_2} \tan \gamma_{\text{prism}}. \tag{9.48}$$

This pulse-front matched interaction geometry results in maximum lateral spatial overlap between the pump and signal while avoiding spatial chirp. Pulse-front matching becomes particularly important in high-energy NOPAs [10], because of the larger pump-beam diameters used, and it can also be realized with gratings instead of prisms.

9.9 Optical parametric chirped-pulse amplification (OPCPA)
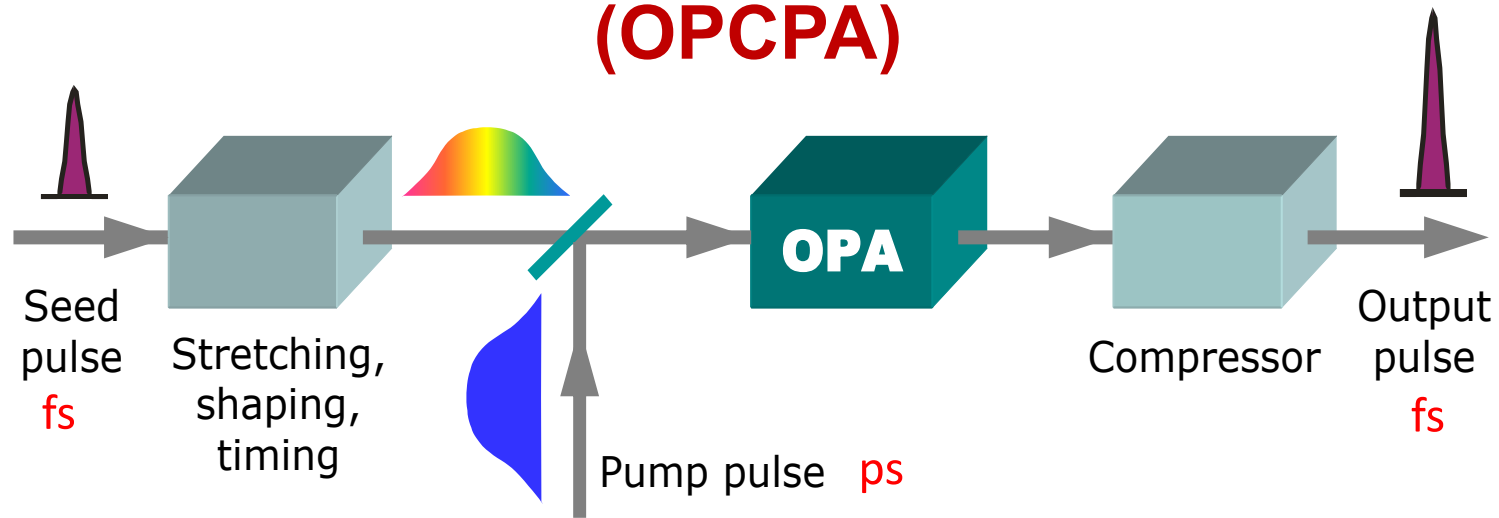
advantages over **stimulated emission based amplifier systems**:

- \+   gain bandwidth can be 'engineered' $\rightarrow$ **other wavelengths**
           (nonlinear crystal, interaction geometry)
- \+   large single-pass gain (10^6-10^7 in millimeters of gain crystals)
- \+   preserves carrier-envelope phase (CEP),
- \+   **passive CEP stabilization** (G. Cerullo *et al.*, Laser & Photonics Rev. **5**, 323 (2011))
- \+   transitions between <u>virtual states</u>
           $\rightarrow$ no energy storage $\rightarrow$ thermal loading not a problem
- \+   **good energy-scalability and repetition-rate scalability** ("next-generation fs sources")

- \-   no pump-energy accumulation (high intensity pump required)
- \-   precise pump-signal synchronization required

200 TW 45 fs laser based on OPCPA
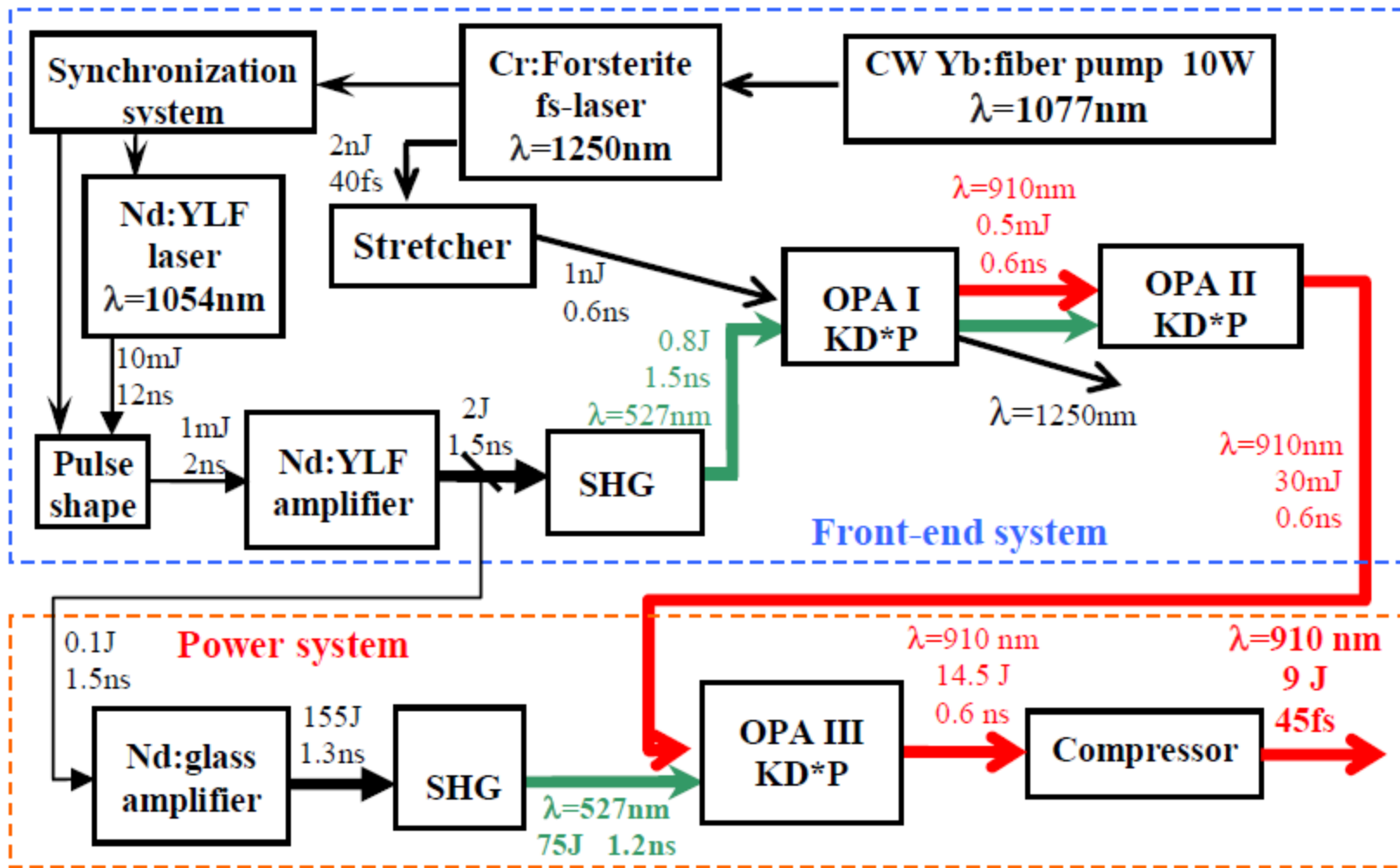
Fig. 1. Scheme of 200TW laser system based on OPAs.

V. V. Lozhkarev *et al.*, Opt. Express **14**, 446 (2006)

1 PW OPCPA using 100 mm LBO (SIOM, 2014)

SULF (Shanghai Superintense Ultrafast Laser Facility)

slide by Ruxin Li (SIOM)

LBO：
100mm×100mm×17mm
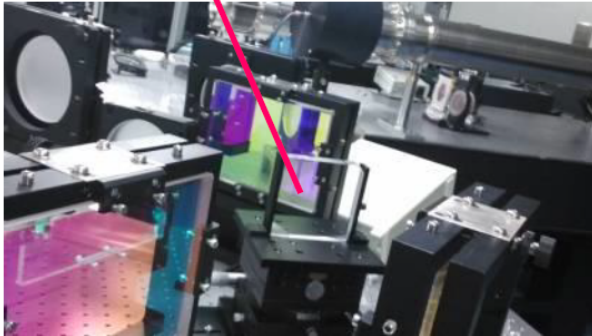
Beam size：
pump：84mm
signal：82mm

Pulse width：
pump：2.89ns
signal：1.9ns
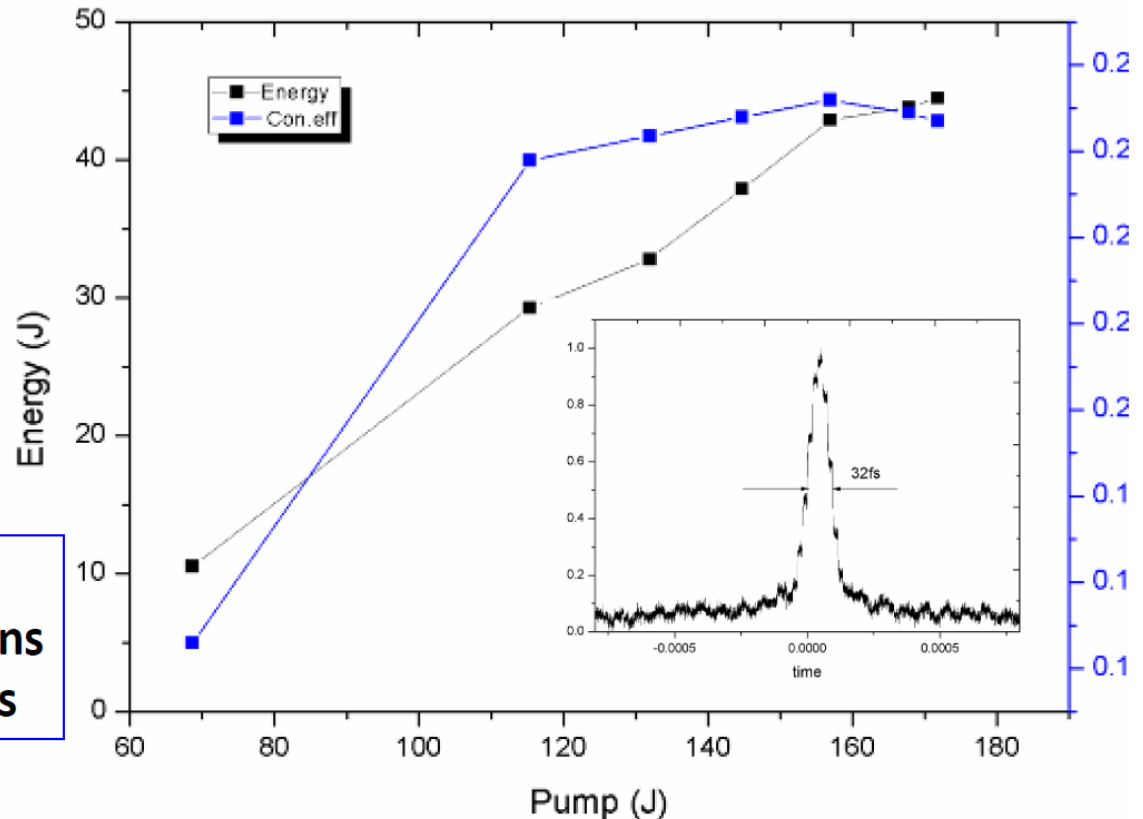
Compressor Effi：72%
Output Energy：32.0J
Pulse Width：32.0fs
Peak Power：1.0PW

Laser Energy：44.5J
Pump Energy：167J
Pump fluence：1.06GW/cm²
Conversion Efficiency：26%

10 PW Ti:sa
CPA booster

L. Yu *et al.*, Opt. Lett. **40**, 3412 (2015)

Optical Parametric Chirped-Pulse Amplifier (OPCPA)

2-μm OPCPA
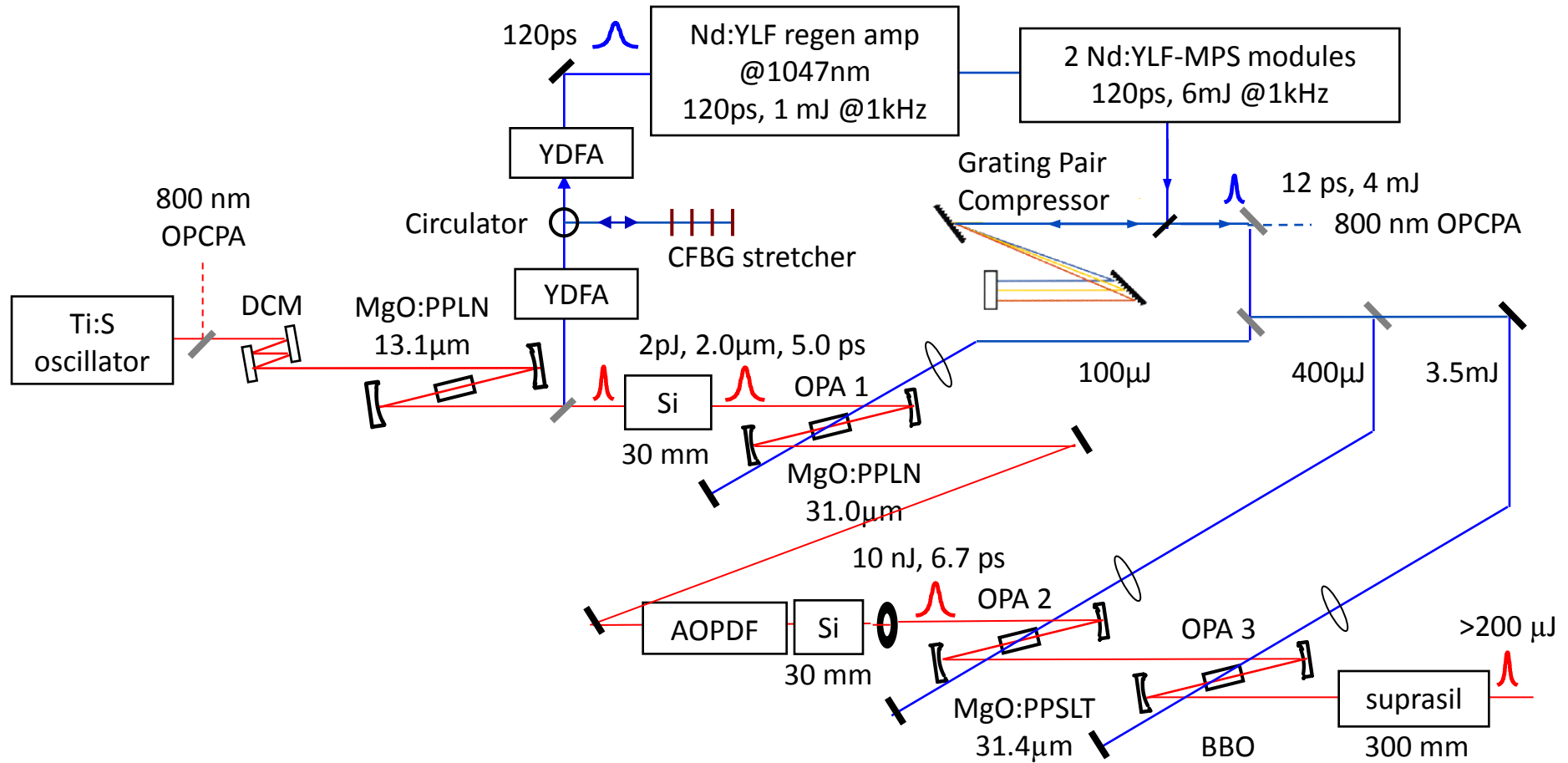
Next-generation high-rep-rate attoscience driver sources

LCLS-II

SCSS

ELI-ALPS (<5fs 5mJ 100kHz)

European XFEL

FLASH
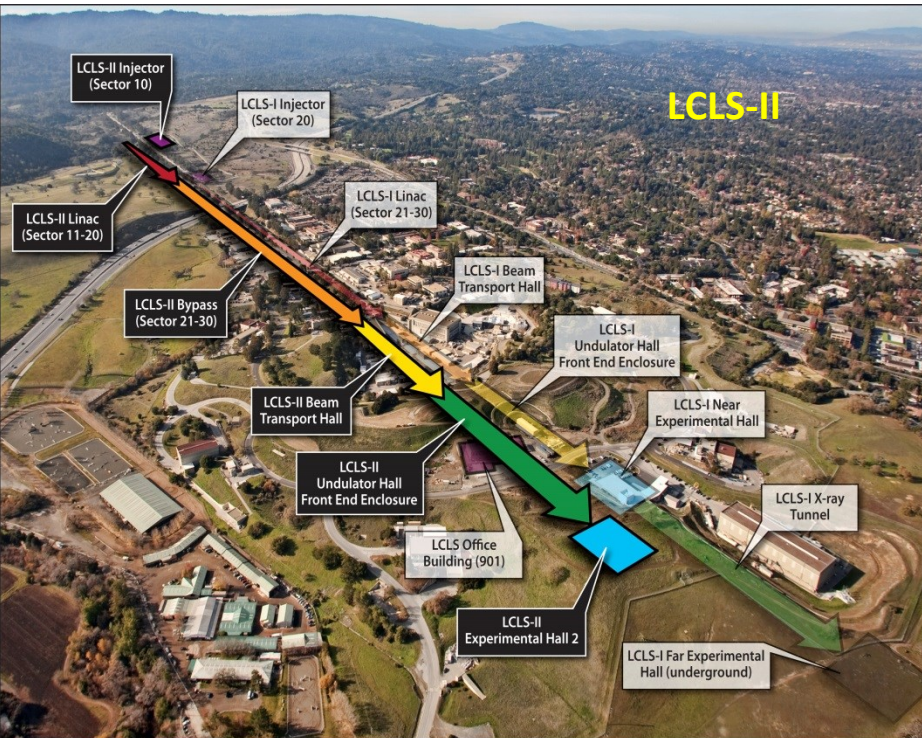
9.9.1   Temporal optimization of ultrabroadband high-energy OPCPA

avoid/suppress parametric superfuorescence buildup in amplification chain

simultaneous optimization of conversion efficiency, signal bandwidth, and signal-to-noise ratio (SNR)

rule of thumb: $\Delta t_s / \Delta t_p$ ranging between 0.2 to ~0.6

noise amplification leads to gain quenching

"case study" by J. Moses *et al.*, Opt. Express **17**, 5540 (2009):

spatio-temporal variation of the small-signal gain

$$g(I_p(t), \Delta k(t))$$

$$\Delta k(t) = k_p - k_s(t) - k_i(t)$$

To gauge the maximum possible conversion efficiency of the amplifier, the concept of the temporal region of significant gain of the pump pulse is useful. Consider parametric amplification of a seed pulse with spectrum centered at signal frequency ω_s by a pump pulse with center frequency ω_p such that $\omega_p = \omega_s + \omega_i$. If the idler is unseeded, prior to significant pump depletion the gain obeys the relation $G = I_s(L)/I_s(0) = 1 + (\Gamma^2/\gamma^2)\sinh^2(\gamma L)$, where $\gamma = \sqrt{\Gamma^2 - (\Delta k/2)^2}$, and $\Gamma^2 = 2\omega_s\omega_i d_{\text{eff}}^2 I_p/n_s n_i n_p \epsilon_0 c^3$. If the gain is reasonably large, i.e., $\Gamma L \gg 1$,

$$G \simeq \frac{1}{4}\exp\left(2\left[\Gamma^2 - (\Delta k/2)^2\right]^{1/2} L\right), \tag{9.49}$$

which, in the case of perfect phase matching, can be recast in the form

$$G \simeq \frac{1}{4}\exp\left(2\Gamma L\right). \tag{9.50}$$

In this case, since $\Gamma \sim \sqrt{I_p}$, the gain is time-dependent and follows the pump pulse intensity profile: $G(t) \sim \exp[\sqrt{I_p(t)}]$. $G(t)$ is plotted in Fig. 9.26(a) alongside $I_p(t)$ for a Gaussian pump pulse and unchirped, phase-matched seed. The peak gain is 100 and the plotted gain profile is normalized to 1. Significant gain will only be possible for a seed pulse overlapped with the pump pulse within a central region around $t = 0$. The shaded interval of Fig. 9.26(a) corresponds to the region $t < |t_g|$ where $G(t) \geq e^{-1}G_0$, with peak gain $G_0 = G(t = 0)$.

13
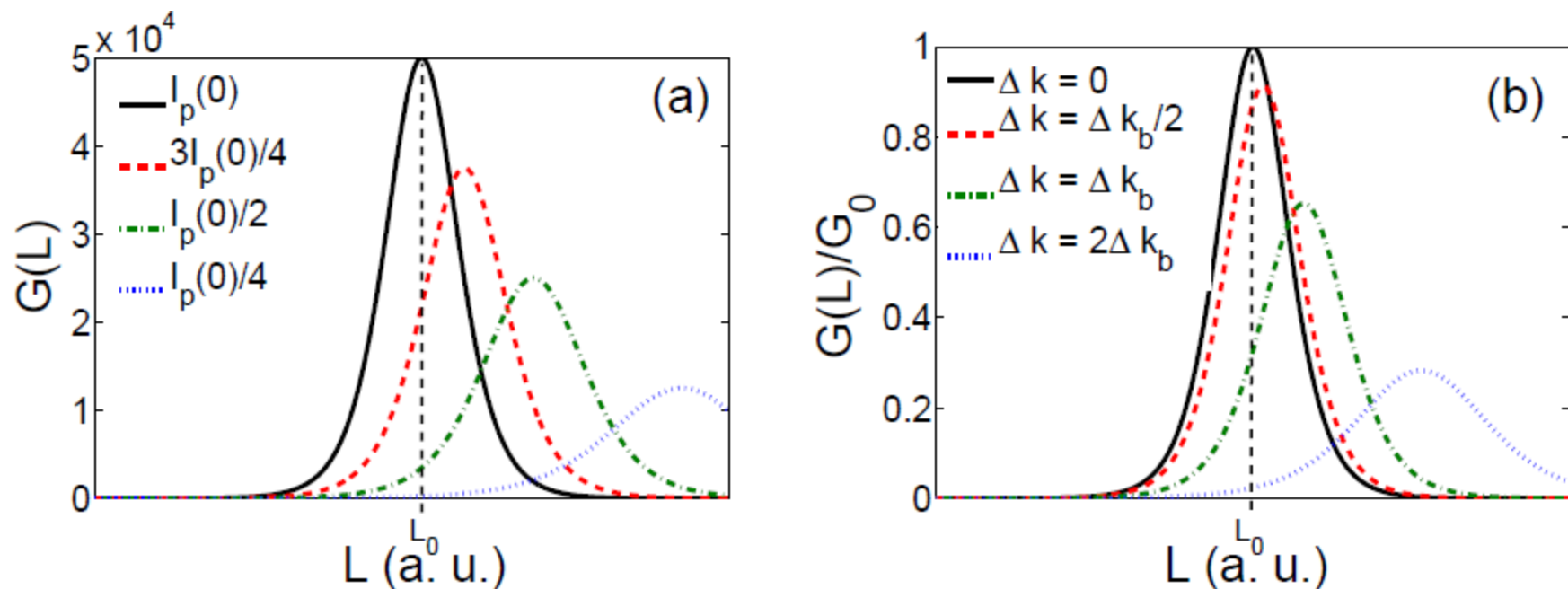
Figure 9.25: Signal gain, G, versus propagation length, L, for a phase-matched ($\Delta k = 0$) parametric amplifier that has a peak gain $G_0 = 5 \times 10^4$, calculated by solution of the coupled nonlinear wave equations describing parametric amplification for monochromatic plane waves. L_0 is the length at which the gain curve peaks with an initial pump intensity $I_p(0)$, i.e., the length at which the pump is fully depleted and before backconversion occurs. In (a), gain curves corresponding to lower pump intensity are also shown (representing, for example, the amplification that occurs along the wings of a pump pulse relative to its peak). In (b), the effect of increasing Δk is shown, with an initial pump intensity $I_p(0)$ for all curves. Δk_b is the wavevector mismatch that reduces the gain at L_0 by $1/e$. [15]

14
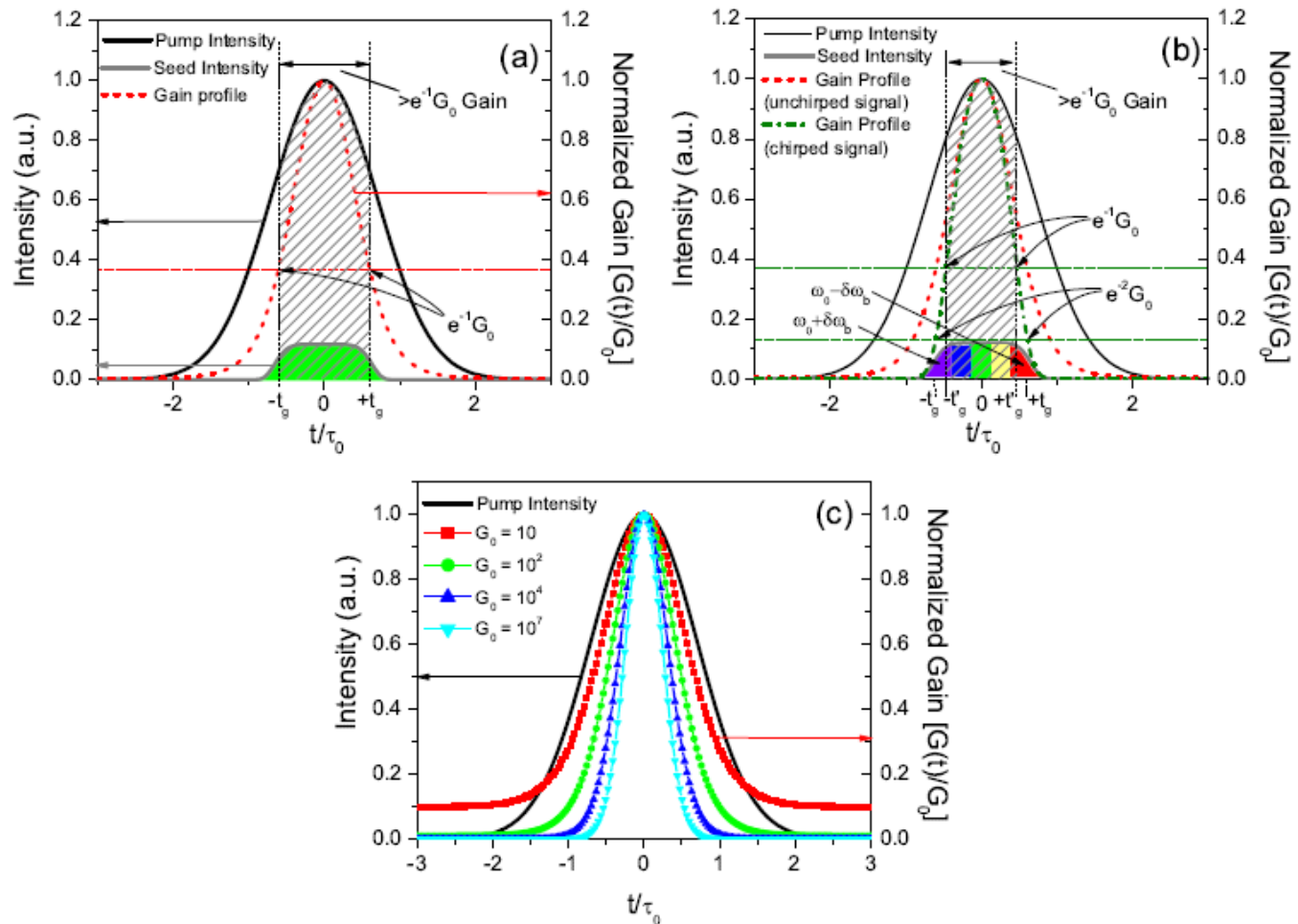
Figure 9.26: (a) Normalized Gaussian pump pulse profile (black, solid) and corresponding temporal gain profile (red, dashed) of an unchirped phase-matched parametric amplifier with a peak gain $G_0 = 100$. The shaded region indicates the region of the pump pulse where gain is $\geq e^{-1}G_0$. A suitable seed pulse is also indicated. (b) The equivalent of (a) but assuming a seed spectrum extending from $\omega_s - \delta\omega_b$ to $\omega_s + \delta\omega_b$ and chirped such that frequencies $\omega_s \pm \delta\omega_b$ just fit within the region of significant gain corresponding to (a). (c) Normalized pump intensity profile and corresponding gain profiles for various values of the peak gain for an unchirped phase-matched amplifier. [15]

15

Let us calculate the centroid bounds, $\pm t_g$, corresponding to a gain $G(t_g) = e^{-1}G_0$, in the case of perfect phase matching. If we define the small-signal gain $g(t) = 2\Gamma(t)L$ and $g_0 = g(0)$, we obtain

$$\frac{g(t_g)}{g_0} = \sqrt{\frac{I_p(t_g)}{I_p(0)}} = \frac{g_0 - 1}{g_0}. \tag{9.51}$$

For a Gaussian pump pulse, described by $I_p(t) = I_0 \cdot \exp(-(t/\tau_0)^2)$ with FWHM duration $\Delta t_p = 2\tau_0 \cdot \sqrt{\ln 2}$, we may rearrange Eq. (9.51) to find

$$t_g = \frac{\Delta t_p}{2\sqrt{\ln 2}}\sqrt{-2\ln\left[1 - 1/\ln(4G_0)\right]}. \tag{9.52}$$

Since pump depletion will typically occur only where there is significant signal gain, t_g thus gives a measure of the maximum possible energy extraction from the pump. Note that t_g is a function of the peak gain G_0, and that a power amplification stage with low G_0 will have a larger gain centroid width than a pre-amplification stage with high G_0. Thus, the power amplier can extract more energy from the pump pulse, resulting in a higher maximum conversion efficiency. Figure 9.26(c) plots the temporal gain profile of an amplifier with unchirped signal pulse for several values of G_0, each curve normalized to 1, and Table 9.1 tabulates the pump centroid width. The difference in t_g for pre- and power amplifiers implies that a different seed pulse chirp will optimize amplification at each stage. For example, a power amplifier stage with $G_0 = 10^2$ has $1.5\times$ wider a region of significant gain than a preamplifier stage with $G_0 = 10^5$.

16

Table 9.1: Width of temporal region of significant gain versus peak gain

G_0	10	10^2	10^3	10^4	10^5	10^6	10^7
$2t_g/\Delta t_p$	0.955	0.725	0.609	0.534	0.483	0.443	0.412
$2t'_g/\Delta t_p$	0.726	0.571	0.483	0.425	0.385	0.353	0.335

For an OPCPA, we need to include also the temporally-varying wavevector mismatch, $\Delta k(t)$. According to Eq. (9.49), wavevector mismatch leads to a reduction in the gain at the wings of the signal pulse if phase-matched at the center of the pulse. In Fig. 9.26(b), the red (dashed) curve represents the gain profile of the unchirped signal pulse of Fig. 9.26(a), while the green (dot-dashed) curve includes the effects of the temporally-varying wavevector mismatch and the resulting decrease in the small-signal gain. The signal pulse is linearly chirped such that the edges of the phase-matching bandwidth, $\omega - \omega_s = \pm\delta\omega_b$, where $G(\omega_s\pm\delta\omega_b) = e^{-1}G(\omega_s)$, are mapped to coordinates $t = \pm t_g$. The new temporal region of significant gain, $-t'_g < t < t'_g$, where $G(t'_g) = e^{-1}G_0$, is narrower.

In principle, as the signal chirp is increased, the region $-t_g < t < t_g$ will on average contain signal frequencies that are closer to the phase-matched frequency; Δk remains small across the bounds and t'_g tends to t_g, increasing the maximum possible conversion efficiency. However, the larger the chirp, the smaller the portion of the signal bandwidth that will fit within the region $-t'_g < t < t'_g$, and thus the smaller the effective amplifier bandwidth. In the other limiting case of vanishingly small chirp, all the seed colors see approximately the peak pump intensity; in this case, t'_g is determined solely by phase matching, and $t'_g \ll t_g$. The bandwidth approaches the full phase-matching bandwidth, but the energy extraction is limited since only a small temporal window of the pump can be depleted.

17

trade-off between **conversion efficiency** and **bandwidth**
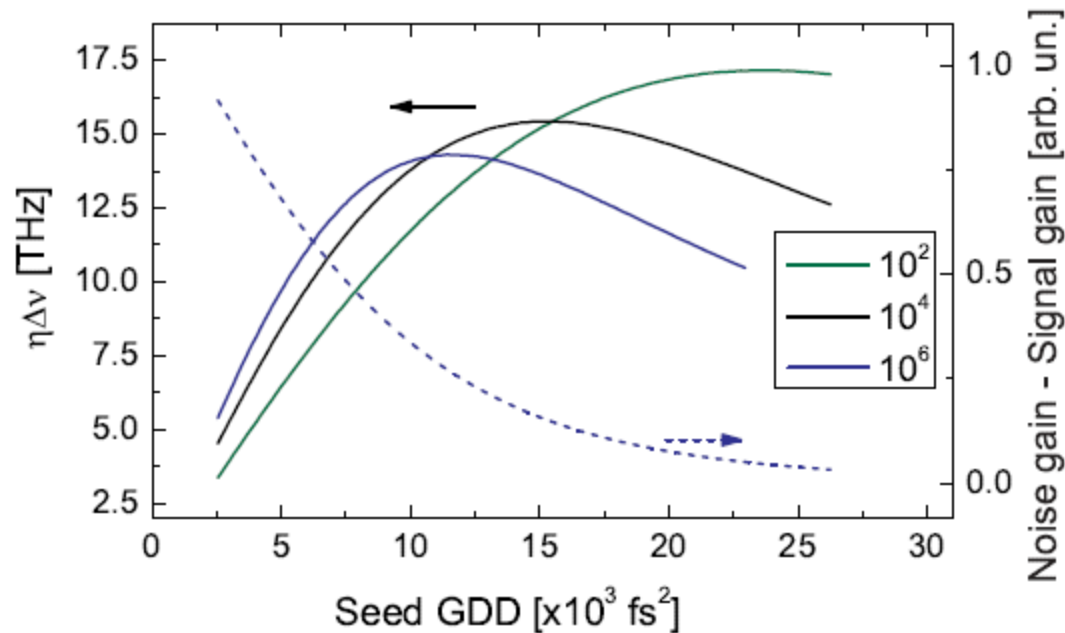
Figure 9.27: (solid lines) Efficiency-bandwidth products, $\eta\Delta\nu$, obtainable from the OPCPA for different values of the seed chirp (GDD) and peak gains of 10^2, 10^4 and 10^6. (dashed curve) Total noise gain subtracted by total signal gain for $G_0 = 10^6$. Curves are calculated for 1.047-μm pump and 2.094-μm signal and idler mixing in 3 mm of PPSLT. The pump is 9-ps long. [15]

chirping seed influences $\Delta k(t)$

optimum chirp depends on G_0 (different in each stage!)

analysis of Eq. (9.49). Figure 9.27 plots the efficiency-bandwidth product calculated from Eq. (9.49) for given values of the peak gain G_0, varying the seed chirp and thus influencing the corresponding mismatch function $\Delta k(t)$. For later comparison, we consider the amplifier materials and geometry that will be discussed in section 3, and operate at degeneracy (i.e., $\omega_s = \omega_i = \omega_p/2$). We approximate the wave-vector mismatch for the broadband amplifier to second-order (with first-order term vanishing due to the matched signal and idler

group velocities) by $\Delta k(\omega) = -(\omega - \omega_s)^2 \beta_2(\omega_s)$, where $\beta_2(\omega_s) = \partial^2 k/\partial \omega^2|_{\omega_s}$ is the material group-velocity dispersion (GVD) evaluated at central signal frequency ω_s. The chirp is linear and each component ω is mapped at $t = (\omega - \omega_s)/\text{GDD}$ (with group-delay dispersion, GDD). Since significant energy extraction from the pump occurs only where there is significant signal gain, *efficiency* was calculated as the fraction of pump energy included in the bounds $-t'_g < t < t'_g$, and the *bandwidth* corresponds to $2\delta\omega_g/2\pi$, where we define $\omega_s \pm \delta\omega_g$ as the frequencies mapped to $t = \pm t'_g$. Figure 9.27 demonstrates a clear optimum chirp for each value of G_0, as expected, since efficiency increases and bandwidth decreases with increasing chirp. In order to compare the gain width of the unchirped, phase-matched amplifier to that of the chirped-pulse amplifier optimized for maximum efficiency-bandwidth product, the values of t'_g corresponding to the optimum chirp at each G_0 are tabulated in the second line of Table 1. The parameters $2t_g/\Delta t_p$ and $2t'_g/\Delta t_p$ exhibit the same behavior as G_0 is varied: larger peak gains result in narrower regions of significant gain. Consistently, $t'_g < t_g$.

SNR degradation due to superfluorescence buildup

amplifier seeded by both signal and quantum noise

signal gain $\neq$ noise gain

initial quantum noise is stationary, i.e., seed fluctuations of all frequencies are present at all times

$\rightarrow$ phase-matched quantum noise is available at all times

noise gain profile is like the signal gain profile of an unchirped, phase-matched amplifier, with $\Delta k = 0$, at all times

local gain of signal and noise photons are different

noise temporal gain profile is determined solely by local pump intensity, while signal temporal gain profile is determined by both local pump intensity and $\Delta k(t)$
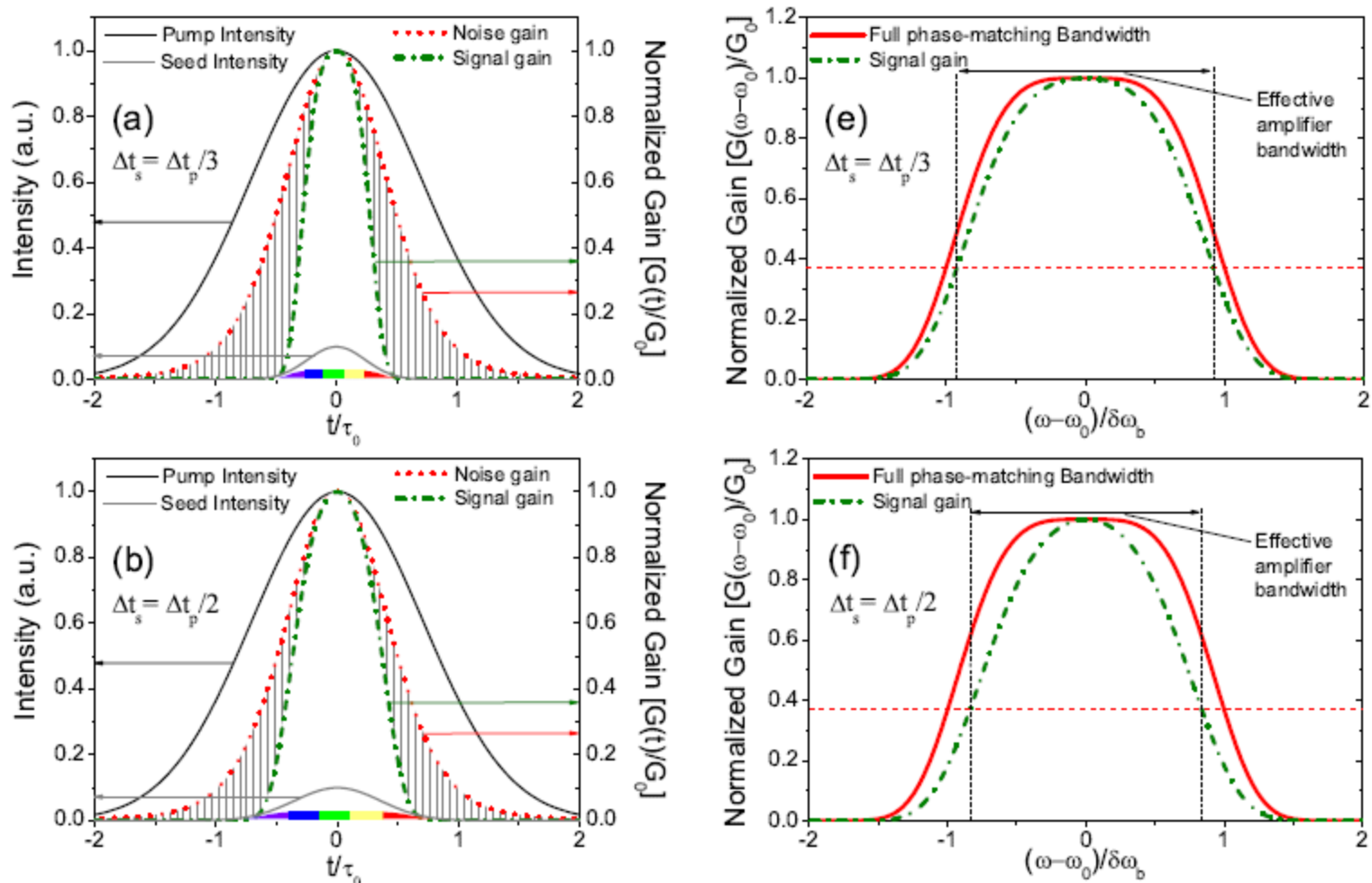
Figure 9.28: (a-d) Gaussian pump (black, solid) and seed (gray, solid) intensity profiles with corresponding signal gain (green, dot-dashed) and noise gain (red, dotted) profiles for several ratios of seed and pump pulse durations ($\Delta t_s/\Delta t_p$). The shaded region represents the difference between noise and signal gain. The chirp of the signal pulse is represented by colored bars. (e-h) Corresponding signal gain profiles (green, dot-dashed) in the frequency domain, plotted alongside the full phasematching bandwidth of the amplifier (red, solid). [15]

Figure 9.28: (a-d) Gaussian pump (black, solid) and seed (gray, solid) intensity profiles with corresponding signal gain (green, dot-dashed) and noise gain (red, dotted) profiles for several ratios of seed and pump pulse durations ($\Delta t_s / \Delta t_p$). The shaded region represents the difference between noise and signal gain. The chirp of the signal pulse is represented by colored bars. (e-h) Corresponding signal gain profiles (green, dot-dashed) in the frequency domain, plotted alongside the full phase-matching bandwidth of the amplifier (red, solid). [15]

J. Moses *et al.*, Opt. Express **17**, 5540 (2009)   (details in manuscript)

modelling of 2.1-µm OPCPA in

J. Moses *et al.*, Opt. Lett. **34**, 1639 (2009)   (discussed later!)

amplifier is pumped by a 9-ps FWHM Gaussian pulse at 1.047 μm and seeded by a broadband pulse at 2.094 μm, for operation around degeneracy. The interaction was calculated in a 3-mm long periodically-poled stoichiometric lithium tantalate (PPSLT) crystal. The seed had a super-Gaussian spectrum $(I_s(\omega) \sim \exp\left[-(\omega - \omega_s)^8\right])$ with FWHM bandwidth of 69 THz, which well matches the 15-fs ($\sim$2-optical-cycle) phase-matching bandwidth of the amplifier. These input parameters are close to the experimental conditions of Ref.
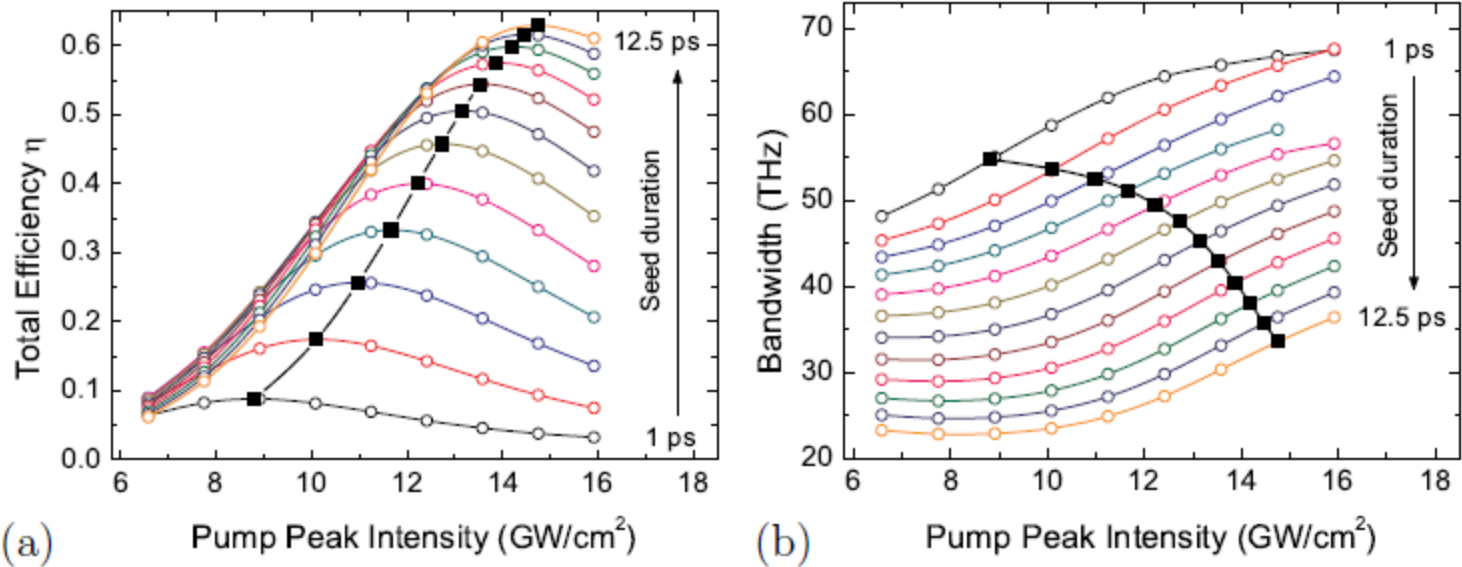
Figure 9.29: Efficiency (a) and bandwidth (b) of the OPCPA process for various seed durations and pump peak intensities, for the case $E_p/E_s = 10^4$. Squares of panel (a) highlight the highest efficiency, η_{max}, obtainable for a given seed duration; the corresponding bandwidths, $\Delta\nu$, are indicated as filled squares in panel (b). [15]

(i) amplified bandwidth decreases with increasing seed pulse duration, due to the progressively lower gain experienced by the wings of the spectrum

(ii) for each seed pulse duration there is an optimum peak intensity that guarantees the highest efficiency [squares in (a)] (higher intensities induce back-conversion at the peak of the pump pulse that exceeds additional conversion at the wings)

(iii) as seed duration is increased, the maximum possible conversion efficiency increases

(iv) for a given seed duration, as the amplifier reaches maximum conversion the bandwidth increases with intensity due to saturation of gain at the center of the pulse and preferential amplification at the wings.
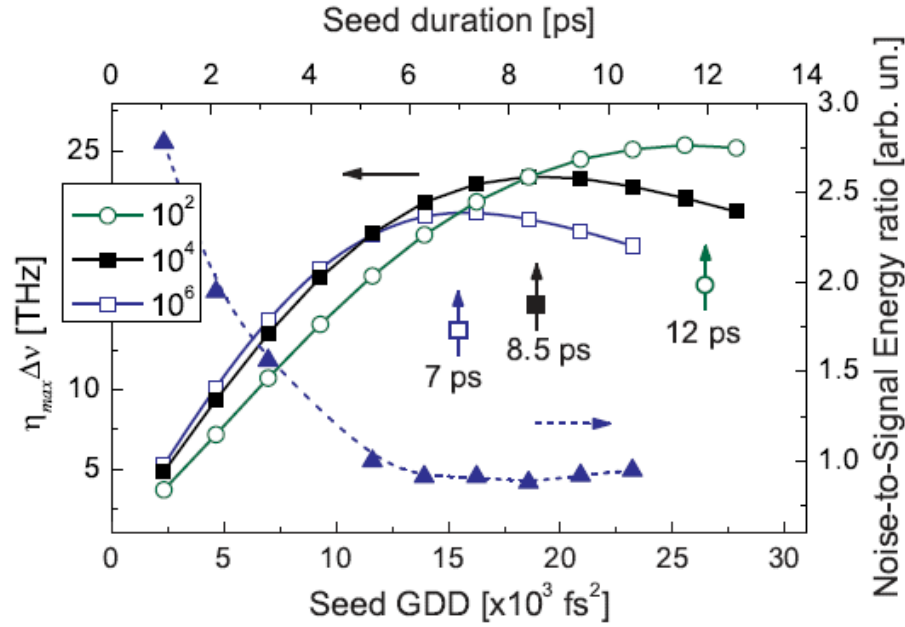
24

Figure 9.30: Best gain-bandwidth products obtainable from the OPCPA for various seed durations and pump-to-signal energy ratios of $E_p/E_s = 10^2$ (circles), $E_p/E_s = 10^4$ (filled squares) and $E_p/E_s = 10^6$ (open squares). The seed durations corresponding to the best performances at the three operating regimes are shown. The increase in noise relative to signal during amplification is shown for the data points of the $E_p/E_s = 10^6$ curve (triangles). [15]

$$(\Delta t_s/\Delta t_p)_{opt} \approx a\sqrt{-2\ln\left[1 - 1/\ln(2E_p/E_s)\right]}, \qquad (9.55)$$

where $a = 2.1$, and therefore $(\Delta t_s)_{opt} \simeq 1.7(2t_g)$. The extra factor of 1.7 can be attributed to the increase in temporal gain profile width due to amplifier saturation: gain at the peak of the pump pulse saturates before gain at the wings does, which pushes out the wings of the gain profile. Even with the effects of saturation, however, the simple non-pump-depletion-regime analysis in the previous section still recovers the scaling of $(\Delta t_s/\Delta t_p)_{opt}$ with E_p/E_s.
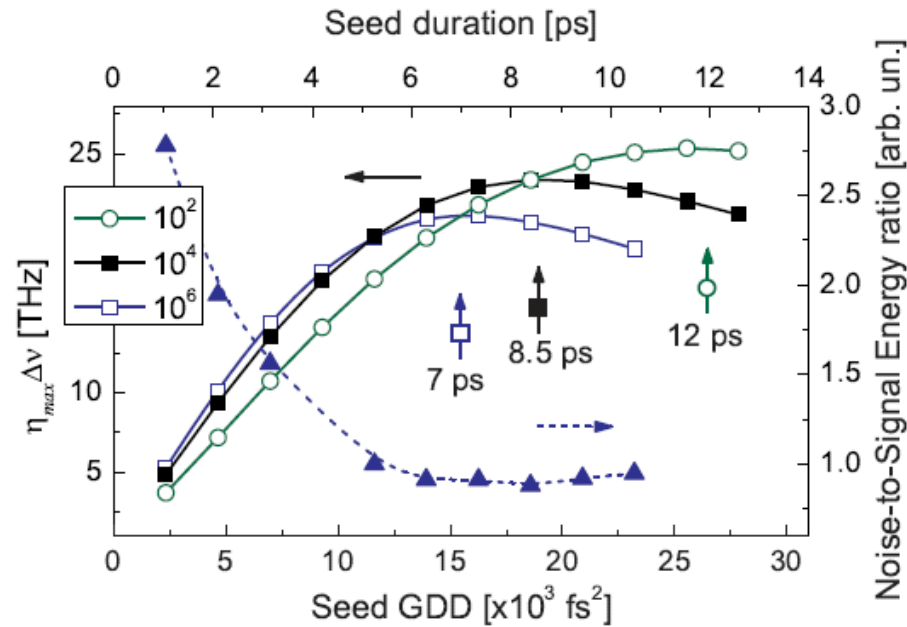
25

Figure 9.30: Best gain-bandwidth products obtainable from the OPCPA for various seed durations and pump-to-signal energy ratios of $E_p/E_s = 10^2$ (circles), $E_p/E_s = 10^4$ (filled squares) and $E_p/E_s = 10^6$ (open squares). The seed durations corresponding to the best performances at the three operating regimes are shown. The increase in noise relative to signal during amplification is shown for the data points of the $E_p/E_s = 10^6$ curve (triangles). [15]

Figure 9.30 plots the calculated degradation of SNR as a function of seed chirp (triangles). As predicted, the SNR performance improves significantly as the seed chirp increases, leveling off at close to the same value that maximizes the efficiency-bandwidth product. This completes the confirmation of a general conclusion of the previous section regarding OPCPA optimization: a small sacrifice in amplifier bandwidth relative to the full phase-matching bandwidth of the amplifier simultaneously allows optimal efficiency-bandwidth product and good robustness of SNR.

numerical result   **experiment**
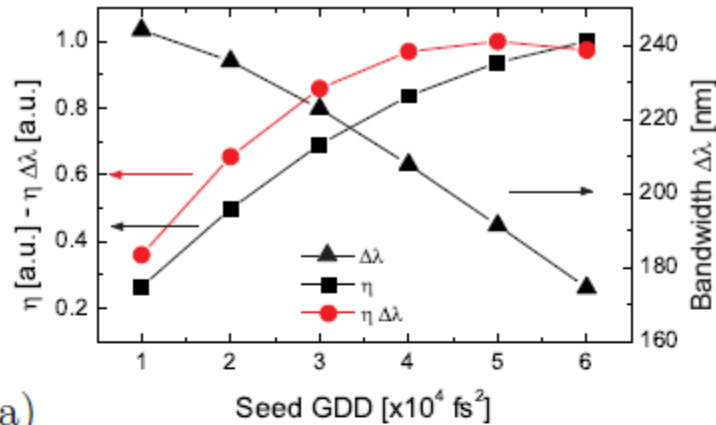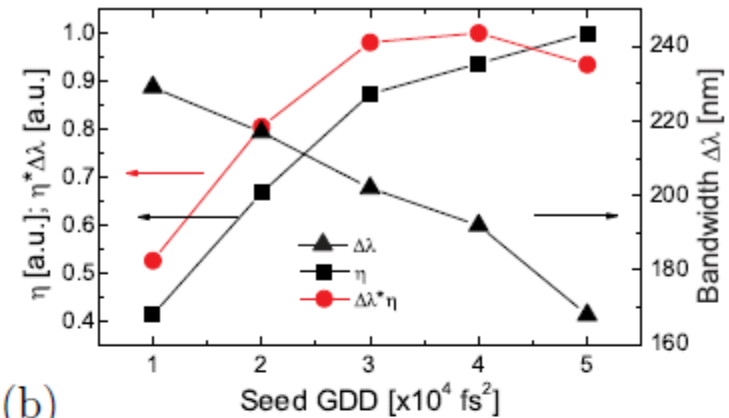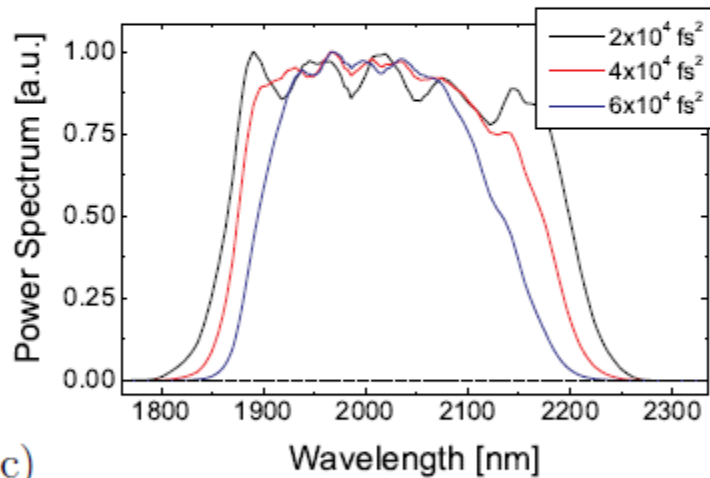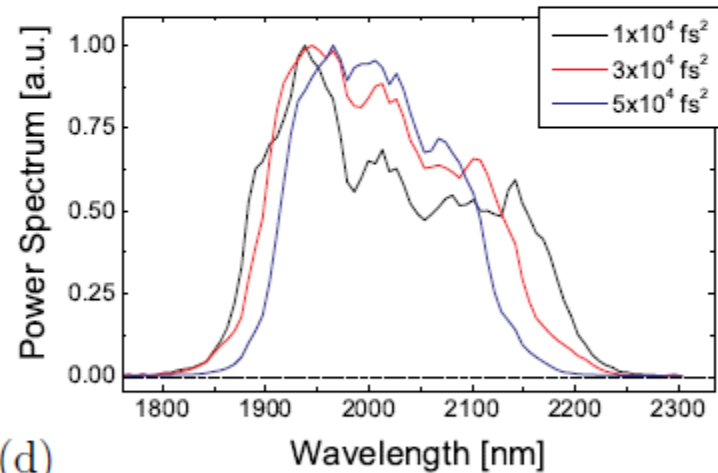
Figure 9.32: Comparison between numerical simulations [(a),(c)] and experiments [(b),(d)] for a 3-mm long, 9-ps pumped, PPSLT-based amplifier. (a)-(b) Best efficiencies and bandwidths as a function of seed chirps. (c)-(d) Amplified spectra corresponding to the maximum efficiencies for the three given seed chirps. [15]

27

Conclusions:

1. simultaneous amplification of signal and background superfluorescence can be treated as simultaneous chirped-pulse and non-chirped-pulse amplification, respectively. Instantaneous signal amplification is sensitive both to the local pump intensity and instantaneous wavevector mismatch, whereas the instantaneous noise amplification is sensitive to only the local pump intensity.

2. crucially important parameter: $\Delta t_s / \Delta t_p$ as seed chirp increases, the maximum conversion efficiency increases, the amplifier bandwidth decreases, and the SNR increases. A small sacrifice in effective amplifier bandwidth relative to the full phase-matching bandwidth of the amplifier can significantly improve the SNR

3. optimal optimum $\Delta t_s / \Delta t_p$ depends on gain.

Practical consequences for OPCPA design:

high-gain parametric amplifier is often split into two or more stages:
pre-amplification: high gain
power ('booster') amplification: relatively low gain
as peak gain decreases, both maximum achievable conversion efficiency and maximum achievable efficiency-bandwidth product increase. Therefore, by placing most of the gain in a pre-amplifier stage, and only 10^2 gain or lower in the final stage, the final peak power of the amplifier can be maximized.

optimize the signal chirp in each stage!!!

(a)
Stretcher:
GDD = α
Pre-amplifier
$G_0 = 10^6$
Power amplifier
$G_0 = 10^2$
Compressor:
GDD = -α

(b)
Stretcher
GDD = α
Pre-amplifier
$G_0 = 10^6$
AOPDF:
GDD = β–α
Power amplifier
$G_0 = 10^2$
Compressor:
GDD = -β
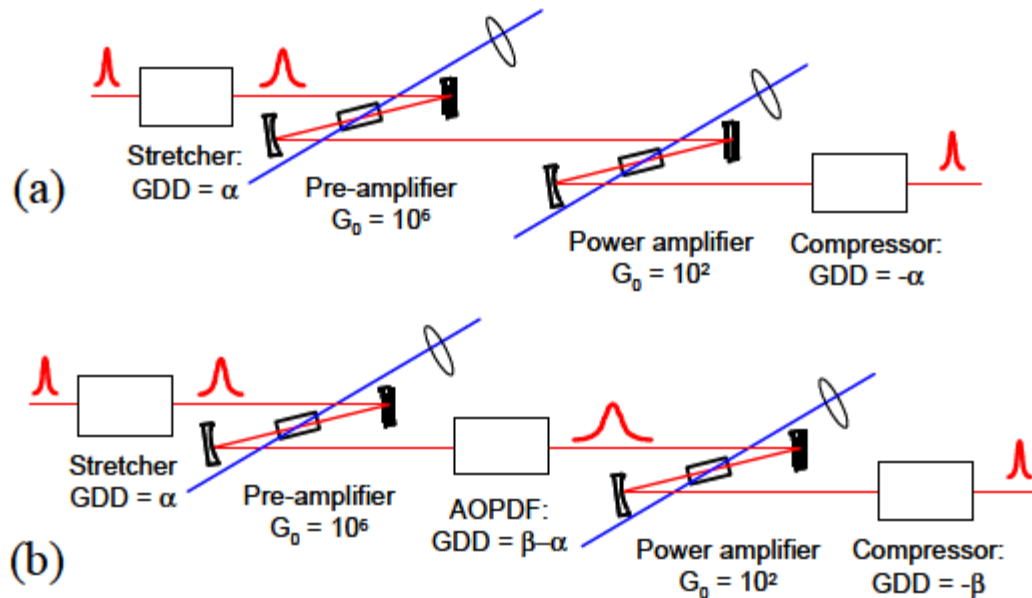
Figure 9.33: Schematics of two-stage OPCPA system designs. In (a), the signal chirp in pre- and power amplifiers must be the same. In (b), a third dispersive element allows independent optimization of $\Delta t_s / \Delta t_p$ at each stage. [15]